Solid State Communications 289 (2019) 51–55

Contents lists available at ScienceDirect

Solid State Communications

journal homepage: www.elsevier.com/locate/ssc

Communication

In-field dependences of the critical current density J_c in $GdBa_2Cu_3O_{7-d}$ coated conductors produced by Zr irradiation and post-annealing at low temperatures

N. Haberkorn[a,b,*], S. Suárez[a,b], Jae-Hun Lee[c], S.H. Moon[c], Hunju Lee[c]

[a] Comisión Nacional de Energía Atómica and Consejo Nacional de Investigaciones Científicas y Técnicas, Centro Atómico Bariloche, Av. Bustillo 9500, 8400 San Carlos de Bariloche, Argentina
[b] Instituto Balseiro, Universidad Nacional de Cuyo and Comisión Nacional de Energía Atómica, Av. Bustillo 9500, 8400 San Carlos de Bariloche, Argentina
[c] SuNAM Co. Ltd, Ansung, Gyeonggi-Do 430-817, South Korea

ARTICLE INFO

Communicated by J. Fontcuberta

Keywords:
A. Coated conductors
D. Critical current densities
E. Ion irradiation

ABSTRACT

We report the influence of 6 MeV Zr^{4+} irradiation and post-irradiation annealing (200 °C) in the in-field dependences of the critical current densities J_c of 1.3 thick $GdBa_2Cu_3O_{7-d}$ coated conductors grown by co-evaporation. Samples were irradiated with 6 MeV Zr^{4+} and fluences between 2.3×10^{11} cm^{-2} and 3×10^{12} cm^{-2}. The correlation between the superconducting critical temperature T_c and in-field dependences of J_c has been analyzed. In addition, random disorder introduced by irradiation was reduced by thermal annealed at 200 °C. The analysis of our experimental findings indicates that the optimal irradiation (reducing random disorder by annealing) results in the suppression of the self-field J_c of ≈10% and in-field J_c enhancements nearly doubled at about 5 T. A clear correlation between T_c, disorder and self-field J_c is observed. Additional random disorder and nanoclusters suppress systematically T_c and increase the flux creep relaxation at intermediate temperatures (reducing the characteristic glassy μ value).

1. Introduction

Artificially designed mixed pinning landscapes seem to be a tool to improve critical current densities J_c in high temperature superconductors [1–3]. A significant enhancement of the in-field J_c of $RBa_2Cu_3O_{7-\delta}$ (*R*BCO; *R*: Sm, Dy, Y, Gd) coated superconductors (CCs) can be obtained by adding pinning centers by ion irradiation [4–8]. For adequate irradiation fluences (which depend on the mass and energy of ions), the addition of small clusters and random disorder assists the pinning produced by normal inclusions and twin boundaries (originated during the synthesis) [9,10]. The optimal doses for irradiation result from a balance between the retention of intrinsic superconducting properties and the enhancement of the vortex pinning. The increment of the disorder at the nanoscale reduces systematically the superconducting critical temperature (T_c) and the self-field J_c. In addition, the decay overtime of the persistent currents (flux creep rates) at intermediate and high temperatures (> 20 K) displays higher values when the irradiation fluency is increased [4–6]. This change in the vortex dynamics has been related to the influence of mixed pinning landscapes in the vortex bundle size [11]. On the other hand, we have recently demonstrated that the reduction in T_c (by changing the oxygen stoichiometry) also increases the flux creep rates in CCs [12].

In this work we study the influence of 6 MeV Zr^{+4} irradiations in the in-field J_c dependences and the vortex dynamics of 1.3 μm thick GBCO films by performing magnetization measurements. For comparison (removal of random disorder), similar measurements were performed after annealing the films at 200 °C for 30 min. The objective of this study is to find a correlation among the disorder produced by irradiation, the T_c and the self-field and in-field dependence of J_c. The pristine films display a pinning landscape with sphere-like and irregular precipitates (Gd_2O_3) embedded in the GBCO matrix with typical diameter of approximately 50 nm [7]. In addition, correlated pinning produced by twin boundaries and boundaries between islands usually assists the pinning produced by the nanoparticles [13]. For proton and oxygen irradiation, the optimal doses result from a balance between the enhancement of the critical current densities J_c and the suppression of the superconducting properties produced by the damage (reduces self-field J_c). Negligible contribution of oxygen vacancies (considered random

* Corresponding author. Comisión Nacional de Energía Atómica and Consejo Nacional de Investigaciones Científicas y Técnicas, Centro Atómico Bariloche, Av. Bustillo 9500, 8400 San Carlos de Bariloche, Argentina.
E-mail address: nhaberk@cab.cnea.gov.ar (N. Haberkorn).

https://doi.org/10.1016/j.ssc.2018.12.008
Received 25 December 2017; Received in revised form 12 November 2018; Accepted 11 December 2018
Available online 12 December 2018
0038-1098/

point defects) to the vortex pinning of pristine 1.3 μm thick GBCO coated conductors was previously observed [12]. Assuming that irradiation with energies of a few MeV produces nanoclusters and random point defects (with larger influence on T_c) [4,6] a question arises: is it possible to increase T_c and maximize vortex pinning (reducing vortex fluctuations) by reducing random disorder? Following this hypothesis, the $J_c(H)$ dependences (5 K, 27 K and 40 K) were measured in GBCO CCs irradiated with 6 MeV Zr^{+4} and then a post-irradiation annealing (200 °C) was done. In addition, the vortex dynamics was analyzed by performing magnetic flux creep measurements.

2. Experimental

The GBCO tape was grown by the co-evaporation technique previously described in Ref. [14]. The magnetization (**M**) measurements were performed by using a superconducting quantum interference device (SQUID) magnetometer with the applied magnetic field (**H**) parallel to the *c*-axis (**H**$\|c$). The J_c values were calculated from the magnetization data using the appropriate geometrical factor in the Bean Model. For **H**$\|$c $J_c = \frac{20\Delta M}{w(1-w/3l)}$, where ΔM is the difference in magnetization between the top and bottom branches of the hysteresis loop, l and w are the length and width of the film ($l > w$), respectively. The measurements were recorded for more than 1 h. The initial time was adjusted considering the best correlation factor in the log-log fitting of the $J_c(t)$ dependence. The initial critical state for each measurement was generated using $\Delta H \sim 4H^*$, where H^* is the field for full-flux penetration [15].

Irradiation with 6 MeV Zr^{+4} is expected to produce random point defects and nm-sized anisotropic defects. Previous irradiation studies of GBCO CCs showed that the optimal dosage to achieve the maximum pinning enhancement at temperatures below 40 K, using either H or O ions are 2×10^{16} cm^{-2} and 1×10^{14} cm^{-2}, respectively [5,7]. However, according to SRIM simulations, the Zr ions will produce significantly more displacements per collision than H or O. Thus, the required dosage should be significantly less. To observe the Bragg-peak inside of the substrate, the Ag cap layer was removed by using chemical etching in an H_2O_2/NH_3 solution (properties such as T_c and J_c are not affected in comparison with samples covered with Ag). The irradiation was performed at room temperature on pieces with typical area 1.2 × 1.2 mm using ion beam currents between 0.15 and 2.4 nA. The samples were irradiated with the ion beam oriented along the crystallographic *c*-axis of the GBCO. To guarantee proper thermal contact, the samples were fixed to the holder with silver paint. The irradiation spot was 1.5 mm in diameter. All the samples displayed similar properties before irradiation. Wherever used, the notation IRRx indicates a GBCO film without irradiation (x = 0), whereas x = 2.3, 3.5, 7, 17, and 30 correspond to films irradiated with Zr^{4+} fluence of 2.3×10^{11} cm^{-2}, 3.5×10^{11} cm^{-2}, 7×10^{11} cm^{-2}, 1.7×10^{12} cm^{-2} and 3×10^{12} cm^{-2}, respectively. After irradiation and for a better comparison of the properties, IRR3.5 and IRR7 were annealed at 200 °C. As no appreciable differences were observed between 30 min and 180 min of annealing, the standard time for this process was established at 30 min. The notation IRRxA corresponds to samples irradiated with doses X and annealed at 200 °C for 30 min.

3. Results and discussions

Fig. 1*a* shows the evolution of T_c for IRR0, IRR3.5, IRR3.5A, IRR7 and IRR7A as determined from the magnetic transition measured in $\mu_0 H = 0.5$ mT (applied after zero-field cooling). Straight lines represent irradiated samples (IRR3.5 and IRR7) and dashed lines, samples annealed at 200 °C (IRR3.5A and IRR7A). Fig. 1*b* shows a summary of the T_c values for all studied films (see also Table 1). As expected, T_c is systematically suppressed when the irradiation fluence is increased. The thermal annealing at 200 °C slightly increases the T_c and also

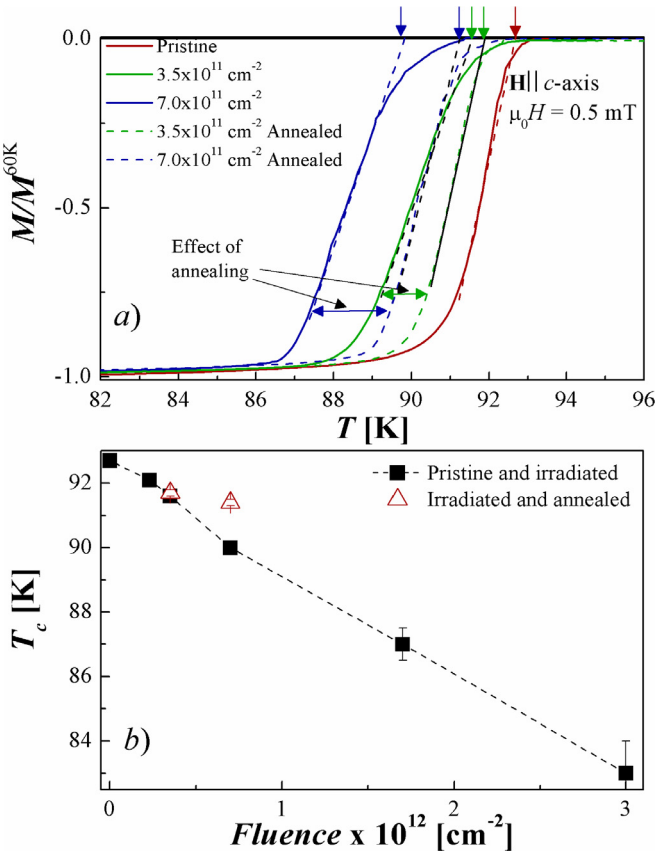

Fig. 1. *a*) Temperature dependence of the magnetization ($\mu_0 H = 0.5$ mT) in the pristine and the irradiated films. The data for the irradiated films after be annealed 200 °C was included. The magnetization value was normalized by its value at 60 K. *b*) Superconducting critical temperature (T_c) versus Zr^{4+} irradiation fluence.

Table 1
Summary of Zr irradiation fluences, superconducting critical temperature (T_c) and glassy exponent μ.

Sample	T_c [K]	μ
Pristine	92.7 ± 0.2	1.63 ± 0.02
IRR2.3 - 2.3×10^{11} cm^{-2}	92.1 ± 0.1	1.60 ± 0.01
IRR3.5 - 3.5×10^{11} cm^{-2}	91.6 ± 0.1	1.52 ± 0.01
IRR7 - 7.0×10^{11} cm^{-2}	90.0 ± 0.1	1.43 ± 0.01
IRR17 - 1.7×10^{12} cm^{-2}	87.0 ± 0.5	1.28 ± 0.02
IRR30 - 3×10^{12} cm^{-2}	83.0 ± 1.0	–
IRR3.5A - 3.5×10^{11} cm^{-2}	91.7 ± 0.1	1.56 ± 0.01
IRR7A - 7×10^{11} cm^{-2} A	91.4 ± 0.1	1.50 ± 0.01

produces an abrupt magnetic flux penetration at the superconducting transition. This can be associated with a reduction of the random disorder, which increases the vortex pinning due to a reduction in the vortex fluctuations close to T_c (associated to variations in λ ($T \rightarrow T_c$) [16]).

Fig. 2 shows on log-log scales the field-dependence of the critical current density J_c (from the Bean model) for IRR0, IRR3.5, IRR7 and IRR17 at 5 K. The results show that an increment in the irradiation fluence systematically decreases $J_c(H \rightarrow 0)$ and produces smooth $J_c(H)$ dependences. With adequate doses (IRR3.5 and IRR7), the in-field dependence of J_c is improved, almost doubled at around 5 T. In addition, the comparison between IRR7 and IRR7A (see inset Fig. 2*a*) shows that thermal annealing increases $J_c(H \rightarrow 0)$ and produces faster decays of $J_c(H)$, which result in similar J_c values at $\mu_0 H = 5$ T. Following, the in-field dependence of J_c (5 K, 27 K and 40 K) will be analyzed. For

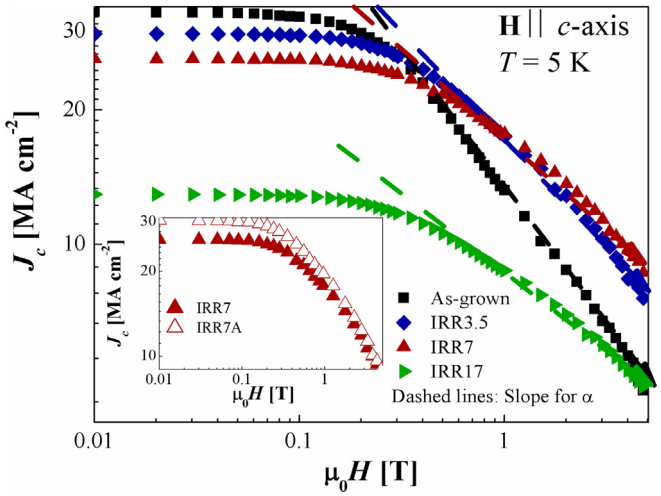

Fig. 2. Magnetic field dependence of the J_c for IRR0, IRR3.5, IRR7 and IRR17 at 5 K. The inset shows a comparison between IRR7 and the same piece annealed at 200 °C for 30 min (IRR7A).

simplicity, J_c (H) dependences at $\approx \mu_0 H > 0.3$ T are approximated as a power-law regime ($J_c \propto H^{-\alpha}$) (see dashed lines in Fig. 2). The deviations of the power-law regime displayed by the irradiated samples could be related to isotropic and anisotropic pinning contributions to J_c [9,17]. The dose dependences of α, $J_c^{H\to 0}$ and J_c^{5T} after Zr irradiation are presented in Fig. 3*a-c*. The results indicate that α decreases with the fluence (≈0.4 for IRR7) and similar changes take place at 5 K, 27 K and 40 K. For IRR7, J_c^{5T} is nearly doubled compared to IRR0, whereas $J_c^{H\to 0}$ is almost 25% lower (i.e. from ≈33 MA cm^{-2} to ≈26 MA cm^{-2} at 5 K). Zr-irradiation fluences higher than IRR7 reduce significantly $J_c^{H\to 0}$ with negligible effect in the α value. The correlation between α and J_c values at small and high magnetic fields is similar to those found in proton and oxygen irradiation [4–7]. Usually, the inclusion of random disorder and nanoclusters makes worse the J_c values at low fields. At this state the vortices remain pinned to the large defects and the systematic $J_c^{H\to 0}$ drop may be attributed to changes in the superfluid density due to an increment in the disorder at the nanoscale [16]. However, the disorder at the nanoscale enhances the vortex pinning at intermediate and high magnetic fields, which is evident from the smooth $J_c(H)$ dependences. For random nanoparticles, when interstitial vortices appear, J_c is expected to vary approximately from $H^{-1/2}$ to H^{-1} [2,18]. Initially, our samples display a pinning landscape with large precipitates (typically 50 nm) and twin boundaries [6], which result in values α ≈ 0.7. After being irradiated, they systematically drop to α ≈ 0.5–0.4. As mentioned in Ref. [12], the oxygen vacancies do not contribute to the vortex pinning in oxygen deficient CCs. In this context, random disorder at IRR3.5 and IRR7 was reduced by thermal annealing in pure oxygen at 200 °C. At this temperature it is expected that random disorder will be removed without affecting the presence of crystalline defects such as the nanoclusters produced by the irradiation [11]. For 5 K, 27 K and 40 K (see Fig. 3*b-c*), the $J_c^{H\to 0}$ values increased (in agreement with an increment in T_c), but the J_c^{5T} was similar to those observed before annealing. This indicates that the disorder removed by the thermal annealing mainly reduces the performance of the CCs at low magnetic fields (where the vortices are mainly pinned by large defects) but has a negligible contribution in magnetic fields above 5 T. At high magnetic fields the presence of nanoclusters introduced by the irradiation assists the pinning produced by the nanoparticles present in the pristine samples [4].

Fig. 4*a* shows the temperature dependence of the normalized logarithmic flux creep rate, $S = -\delta \ln J_c / \delta \ln t$, at $\mu_0 H = 0.5$ T for various irradiation fluences. The irradiation mainly produces an increment in the $S(T)$ values at intermediate and high temperatures [4–7]. The

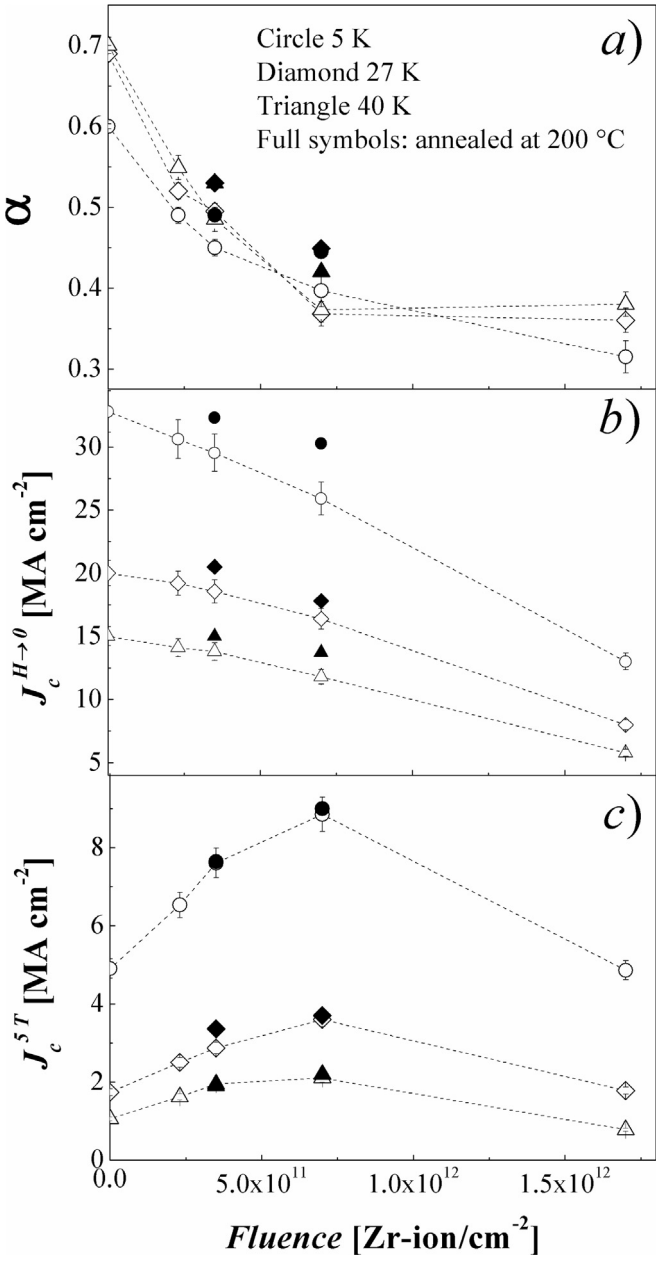

Fig. 3. *a*) α versus Zr fluence obtained from $J_c(H) \propto H^{-\alpha}$ at intermediate and high fields (see Fig. 2). *b-c*) Self-field J_c and J_c^{5T} versus Zr fluence (for 5 K, 27 K and 40 K), respectively. Error bars due to uncertainty in the area are not included for the annealed pieces.

qualitative features of the $S(T)$ curves are similar to previous observations in RBCO [15]. The initial increase of $S(T)$ corresponds to an Anderson-Kim like creep with $S \approx T/U$, where U is the activation energy (approximately T-independent at low T). The IRR0 displays a peak at $T \approx 20$ K, usually attributed to correlated disorder (such as twin boundaries) [9], but which also can be attributed to changes in the strong pinning regimes for nanoparticles [19]. Above the peak, the $S(T)$ relaxation displays a minimum which is usually attributed to glassy relaxation with values determined by the vortex bundle size. Irradiation systematically suppresses the peak at $T \approx 20$ K. Furthermore, at low temperatures, it provokes a reduction in the S values whereas it has a contrary effect at intermediate and high temperatures. According to the collective creep theory, the dynamics in a glassy vortex phase [20] is described by an effective activation energy as a function of current density (J) $U_{eff} = \frac{U_0(T)}{\mu}[(\frac{J_c}{J})^{\mu} - 1]$ [1], where $U_0(T) = U_0 G(T)$ is the

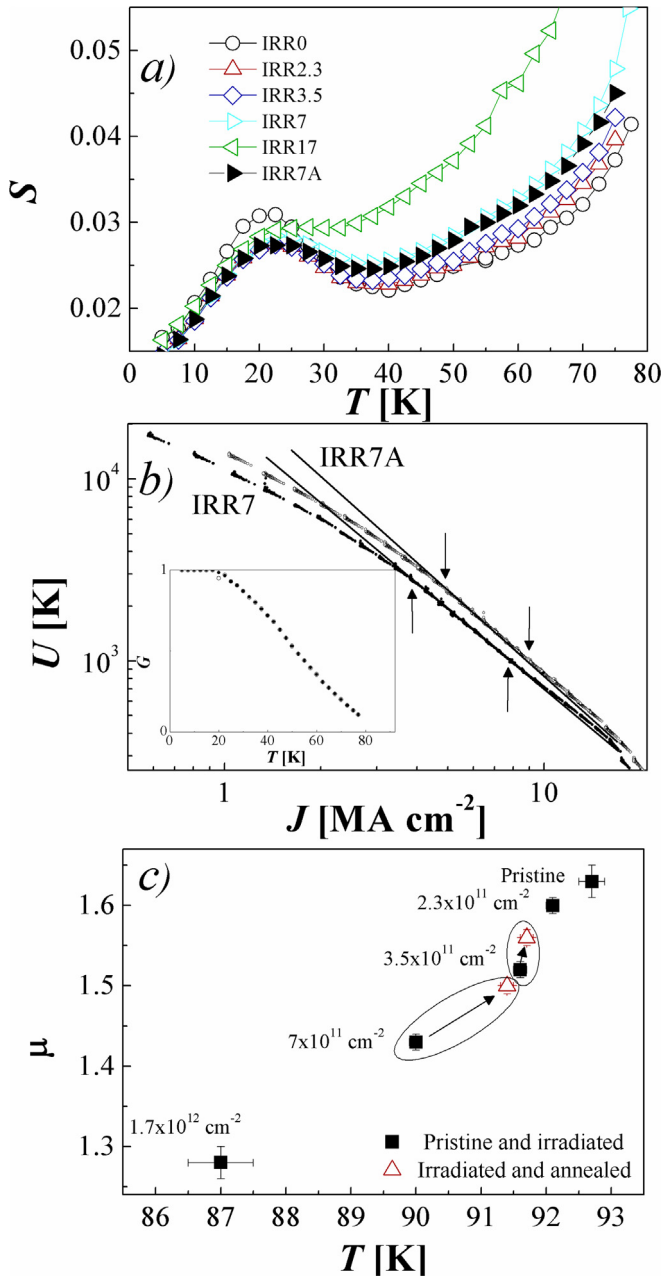

Fig. 4. *a*) Temperature dependence of the creep flux rate (S) at $\mu_0 H = 0.5$ T for IRR0, IRR2.3, IRR3.5, IRR7, IRR17 and IRR7A. *b*) Maley analysis at $\mu_0 H = 0.5$ T for IRR7 and IRR7A. The inset shows the $G(T)$ dependence used for the Maley analysis. *c*) Correlation between T_c and the glassy exponent μ.

scale of the pinning energy, U_0 is the collective pinning barrier at $T = 0$ in the absence of a driving force, $G(T)$ contains the temperature (T) dependence of the superconducting parameters, and $\mu > 0$ is the regime-dependent glassy exponent determined by the bundle size and vortex lattice elasticity. From eq. [1], the temperature dependence of the creep rate (S) results in $S = -\frac{d(\ln J)}{d(\ln t)} = \frac{T}{U_0 + \mu T \ln(t/t_0)} = \frac{T}{U_0}(\frac{J}{J_c})^{\mu}$ [2], where t_0 is a vortex hopping attempt time. This equation predicts that, with increasing temperature, the second term in the denominator dominates U_0, and S approaches the limit $S \approx \frac{1}{\mu \ln t/t_0}$ [15]. Based on the model of nucleation of vortex loops, for random point defects in the three-dimensional case, μ is 1/7, 3/2 or 5/2, and 7/9 for single vortex, small-bundle and large-bundle creep, respectively [19]. The effective activation energy $U_{eff}(J)$ can be experimentally obtained considering the approximation in which the current density decays as $\frac{dJ}{dt} = -(\frac{J_c}{\tau})e^{-\frac{U_{eff}(J)}{T}}$. The final equation for the pinning energy is $U_{eff} = -T[ln|\frac{dJ}{dt}| - C]$ (with C, a constant factor) [21]. For an overall analysis it is necessary to consider $G(T)$, which results in $U_{eff}(J, 0) \approx U_{eff}(J, T)/G(T)$ [22]. Fig. 4*b* shows the Maley analyses for IRR7 and IRR7A. Similar analyses were performed for all studied samples. The inset corresponds to the used $G(T)$ dependence. In the limit of $J \ll J_c$ the μ exponent can be estimated as $\Delta \ln U(J)/\Delta \ln J$ [23]. Fig. 4*c* shows the correlation between μ and T_c. In addition, the μ values obtained at intermediate temperatures are summarized in Table 1. Initially, IRR0 displayed a $\mu = 1.63$ that systematically decreased to 1.28 for IRR17. The μ value observed in the pristine sample is similar to those observed in other CCs [24]. The variations in the μ values for irradiated samples have been related to the influence of mixed pinning landscapes in the vortex bundle size [11]. However, variations in the superfluid density and changes in the anisotropy due to the reduction in T_c (increment in the disorder at the nanoscale) could also contribute to the changes in the vortex dynamics. The thermal annealing reduces the disorder and increases the T_c, which is manifested in a slight increment in μ with values between irradiated and pristine samples.

Finally, the influence of the flux creep rates in the single vortex regime (SVR) will be analyzed. SVR refers to negligible vortex-vortex interaction compared to vortex-defect interaction [20]. The pinning in type II superconductors may originate in disorder in T_c (δT_c) and/or from the spatial variation in the free path l near a lattice defect (δl) [25]. In the SVR, J_c can be expressed as function of the temperature as $J_c \propto (1 - (\frac{T}{T_c})^2)^n$, where the exponent n indicates the type of pinning, being 7/6 and 5/2 for δT_c and δl pinning, respectively [26]. Intermediate values have been observed for mixed pinning landscapes (depending on nanoparticle size and density). For example, in YGd-$Ba_2Cu_3O_y$ films grown by metal organic deposition, $n = 1.24$ and 1.55 for nanoparticles with diameters of ≈20 nm and ≈90 nm, respectively. Fig. 5 shows J_c vs. $(1 - (\frac{T}{T_c})^2)$ at $\mu_0 H = 0.1$ T, the data fit with $n = 1.55$ for IRR0, and systematic shift to $n = 1.76$ for IRR7. The $n = 1.55$ value approximates to what would be theoretically expected for δT_c pinning, and the systematic increment in n seems indicative of larger contribution of random disorder to the pinning (δl). This fact can be related to the pinning for the vortex segments between large nanoparticles, which interacts mainly with small defects produced by the irradiation and produces poorer retention in J_c (T) (possibly associated to larger thermal fluctuations by local changes in the penetration depth λ).

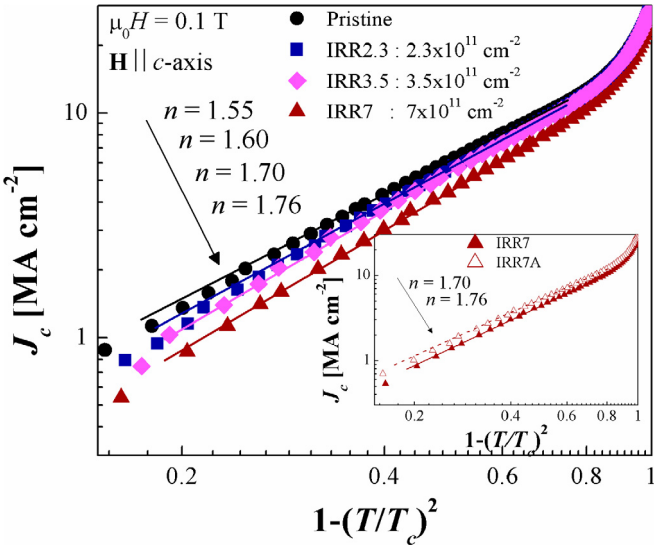

Fig. 5. Log-log plot of J_c vs $(1 - (\frac{T}{T_c})^2)$ for the samples indicated in the panel at $\mu_0 H = 0.1$ T. The inset shows a comparison between IRR7 and the same piece annealed at 200 °C for 30 min (IRR7A).

Thermal annealing reduces the contribution of random point disorder to vortex pinning, which is evident from the shift of n to intermediate values between pristine and irradiated samples (see Inset Fig. 5 for IRR7 and IRR7A).

4. Summary

We examined the influence of 6 MeV Zr^{+4} irradiation in the in-field dependences of the critical current densities J_c of 1.3 μm thick GBCO coated conductors grown by co-evaporation. The results show that the optimal fluence to enhance the in-field dependence is around 7.0×10^{11} cm^{-2}. For this fluence and in comparison with the pristine film, the J_c^{sf} is reduced to around 25% (from ≈33 MA cm^{-2} to ≈ 26 MA cm^{-2} at 5 K), whereas its value is nearly doubled at about 5 T. Thermal annealing at 200 °C reduces the random disorder and the T_c is increased. After annealing and at 5 K, J_c^{sf} is increased to ≈30 MA cm^{-2}, which indicates a large contribution of random disorder to the suppression of the J_c values at low fields. However, at high magnetic fields (i. e. $\mu_0 H = 5$ T), the J_c values remain close to twice the magnitude of the pristine sample, which indicates a significant contribution to the vortex pinning of the nanoclusters produced by the irradiation. For all the analyzed irradiated fluences, larger contribution of random disorder and increment of pinning associated with fluctuations in the mean free path (δl) were observed. The optimal irradiation (considering reduction of random disorder by annealing) results in the suppression of the J_c^{sf} of ≈10% and J_c enhancements almost doubled at about 5 T. A clear correlation between T_c, disorder and J_c^{sf} is observed. In addition, at intermediate temperatures, the flux creep relaxation is systematically affected by the suppression in T_c and by the presence of random disorder, which reduces the characteristic glassy μ value.

Acknowledgement

We thank C. Olivares for technical assistance. This work has been partially supported by ANCYPT PICT 2015–2171. NH is member of the Instituto de Nanociencia y Nanotecnología, CNEA-CONICET.

References

[1] A.E. Koshelev, I.A. Sadovskyy, C.L. Phillips, A. Glatz, Phys. Rev. B 93 (2016) 060508 (5pp).
[2] R. Willa, A.E. Koshelev, I.A. Sadovskyy, A. Glatz, Supercond. Sci. Technol. 31 (2018) 014001 (20pp).
[3] Wai-Kwong Kwok, et al., Rep. Prog. Phys. 79 (2016) 116501 (39pp).
[4] Y. Jia, et al., Appl. Phys. Lett. 103 (2013) 122601 (5pp).
[5] N. Haberkorn, et al., Supercond. Sci. Technol. 28 (2015) 125007 (7pp).
[6] M. Leroux, et al., Appl. Phys. Lett. 107 (2015) 192601 (5pp).
[7] N. Haberkorn, et al., Phys. C 542 (2017) 6–11.
[8] I.A. Sadovskyy, et al., Adv. Mater. 28 (2016) 4593–4600.
[9] M. Miura, et al., Phys. Rev. B 83 (2011) 184519 (8pp).
[10] D. Abraimov, et al., Supercond. Sci. Technol. 28 (2015) 114007 (8pp).
[11] S. Eley, et al., Supercond. Sci. Technol. 30 (2017) 015010 (13pp).
[12] N. Haberkorn, et al., Supercond. Sci. Technol. 30 (2017) 95009 (6pp).
[13] N. Haberkorn, et al., Supercond. Sci. Technol. 29 (2016) 075011 (6pp).
[14] J.L. MacManus-Driscoll, et al., Apl. Mater. 2 (2014) 086103 (8pp).
[15] Y. Yeshurun, A.P. Malozemoff, A. Shaulov, Rev. Mod. Phys. 68 (1996) 911–949.
[16] N. Basov, et al., Phys. Rev. B 49 (1994) 12165–12169.
[17] X. Obradors, T. Puig, S. Ricart, M. Coll, J. Gazquez, A. Palau, X. Granados, Supercond. Sci. Technol. 25 (2012) 123001 (32pp).
[18] A.E. Koshelev, A.B. Kolton, Phys. Rev. B 84 (2011) 104528 (13pp).
[19] Martin W. Rupich, et al., IEEE Trans. Appl. Supercond. 26 (2016) 6601904.
[20] G. Blatter, et al., Rev. Mod. Phys. 66 (1994) 1125–1388.
[21] M.P. Maley, J.O. Willis, H. Lessure, M.E. McHenry, Phys. Rev. B 42 (1990) 2639–2642.
[22] J.G. Ossandon, et al., Phys. Rev. B 46 (1992) 3050–3058.
[23] J.R. Thompson, et al., Phys. Rev. Lett. 78 (1997) 3181–3184.
[24] O. Polat, et al., Phys. Rev. B 84 (2011) 024519 (13pp).
[25] R. Griessen, et al., Phys. Rev. Lett. 72 (1994) 1910–1913.
[26] A.O. Ijaduola, et al., Phys. Rev. B 73 (2006) 134502 (9pp).